

## **Alternative Design of One-Sided Shewhart Control Charts for the Multivariate Coefficient of Variation**

**XinYing Chew**

*School of Computer Sciences, Universiti Sains Malaysia, 11800 USM, Penang*

### **ABSTRACT**

The control charting technique is an approach to quality control and was implemented in various industries. There are many control charts, where the coefficient of variation control chart was one of the common charts and greatly used in Statistical Process Control. Since most processes are multivariate, the multivariate coefficient of variation charts has received great attention in the past few years. However, the existing multivariate coefficient of variation control charts was evaluated in terms of the average run length criterion, which may misinterpret the actual performance of the charts. This paper designs an alternative for the Shewhart multivariate coefficient of variation chart by considering the median run length and expected median run-length criteria to circumvent this problem. The research on the multivariate coefficient of variation chart is very limited in the existing literature by considering the median run length criterion. This proposed chart in this paper can minimize this research gap. The formulas and algorithms of the proposed chart are presented. The outputs of the proposed charts are shown by examining the different upward and downward process shifts. Additionally, the sample sizes, the process shifts, and the variation of the run-length distribution are investigated for their effects on the proposed chart. The findings

reveal that the run-length distribution's variation is inversely proportional to the shift size. Furthermore, it shows that the variation decreases if the shift size increases.

### ARTICLE INFO

*Article history:*

Received: 15 April 2022

Accepted: 20 June 2022

Published: 27 December 2022

DOI: <https://doi.org/10.47836/pjst.31.1.35>

*E-mail address:*

[xinying@usm.my](mailto:xinying@usm.my) (XinYing Chew)

*Keywords:* Control chart, median run length, multivariate coefficient of variation, statistical process control

## INTRODUCTION

The control chart is frequently used in Statistical Process Control for detecting the processed signal. Implementing the control chart aims to improve the quality of processes in various domains such as healthcare, manufacturing, and service (Mim et al., 2019). The traditional control chart was used to monitor the process location and dispersion. Note that the process mean needs to be constant, and the process standard deviation is not correlated to the mean (Khaw & Chew, 2019). Shewhart  $\bar{X}$  was proposed to monitor the process mean, while  $R$  and  $S$  charts are commonly used for process variability. In the past two decades, the coefficient of variation (CV) chart has been widely applied in different domains, where the most common domains are manufacturing, healthcare, finance, and service. The CV can be defined as the ratio of the standard deviation to the mean, and it can be used when the mean and standard deviation of the data are highly correlated. For example, Chanda et al. (2018) investigated the CV obtained from Vegetarian Indices with the millable stalk of sugarcane varieties and plant population. Huang and Tang (2007) proposed a new infrared device for the CV in yarns. Shriberg et al. (2003) used the CV as a diagnostic marker for childhood apraxia of speech, while Alharbi et al. (2019) combined the CV and normalized-difference vegetative index to predict the plant populations in corn. The CV of the endothelial cell area was examined by Doughty and Aakre (2008). The CV is also recently applied in the chemical reactor process (Mahmood & Abbasi, 2021) and continuous glucose monitoring (Mo et al., 2021), respectively.

Kang et al. (2007) were the first researchers to develop the Shewhart CV chart. It could be applied for monitoring the process in which the traditional  $\bar{X}$  and  $R$  charts could not function well. Most traditional charts focus on monitoring the process's mean or standard deviation. However, in some processes, such as the healthcare process, the mean and the standard deviation are not independent, where the mean is not constant and/or the standard deviation is a function of the mean. In such processes, the use of traditional charts is dubious. In these conditions, it is better to monitor the CV. Over the years, many intermediate and advanced CV charts have been discussed by using different strategies, such as exponentially weighted moving average (EWMA) (Zhang et al., 2014; Castagliola et al., 2011), CUSUM (Tran & Tran, 2016), synthetic (Calzada & Scariano, 2013; Chew et al., 2021), run rules (Castagliola et al., 2013), adaptive schemes (Khaw et al., 2017; Castagliola et al., 2015; Yeong et al., 2018) and variable sample size run sum (Yeong et al., 2022). Those proposed charts provided better performance in detecting small and moderate shifts. However, at the same time, the computational difficulties and costs increased.

All preceding charts are used for monitoring the univariate process. In real-life applications, most process monitoring is in multivariate conditions, containing at least two quality characteristics. Yeong et al. (2016) introduced a CV chart in a multivariate case called a multivariate coefficient of variation (MCV). The proposed chart only performs

well when detecting large process shifts. Khaw et al. (2019) and Chew et al. (2020) proposed a synthetic MCV and run rules MCV charts to improve the detection of small and moderate shifts. The results show that the synthetic MCV chart outperformed the Shewhart MCV and run rules MCV charts for detecting small and moderate MCV shifts. However, the drawback of the synthetic MCV chart is its weak efficiency in detecting downward shifts. The adaptive schemes were incorporated into the Shewhart MCV chart to improve performance. Those are variable sampling interval MCV (Nguyen et al., 2019), variable sample size MCV (Khaw et al., 2021), variable sample size and sampling interval MCV (Khaw et al., 2018), and variable parameter MCV charts (Chew et al., 2019). Comparing those adaptive charts reveals that the variable parameter MCV chart provides the best performance detecting small to large shifts in different shift sizes and ranges. More recently, Giner-Bosch et al. (2019) recommended the MCV-squared EWMA chart. More recently, Adegoke et al. (2022) suggested an MCV chart for high-dimensional processes, while Ng et al. (2022) investigated the MCV chart in terms of economic criterion.

To date, the design of the existing MCV charts is based on the average run length (ARL) criterion. According to Khoo et al. (2012), the ARL performance measure should not be the only measure as it could potentially cause the chart's misinterpretation. In addition, the ARL performance measure may not be practically effective due to the inconsistency and excessive variations of the run-length distribution (Zhou et al., 2012). Zhou et al. (2012) stated that the run-length distribution's percentile effectively summarizes the run-length behavior and provides more information on the control chart. Therefore, the 50<sup>th</sup> percentile, also called median run length (MRL), is considered more practical in designing the control chart.

In contrast, the fifth (5%) and 95<sup>th</sup> (95%) percentiles can be used with the MRL for investigating the skewness and spread of the run-length distribution (Chakraborti, 2007). Some of the research works on control charts could be found using MRL. For example, Teoh et al. (2017) proposed a variable sample size chart for monitoring the process mean based on the MRL criterion. The results revealed that the proposed chart performed better than the Shewhart chart. This study is then adopted by Lim et al. (2019) for recommending a variable sample size univariate CV chart. The distribution of CV is investigated in this study. Yeong et al. (2021) recently adopted the side-sensitive synthetic scheme to the CV chart. The proposed chart is more sensitive than the variable sample size CV chart detecting small and moderate CV shifts. With the salient properties of the MRL performance measure, this paper proposes two one-sided Shewhart MCV charts based on the MRL and expected median run length (EMRL). MRL is the median number of samples (subgroups) that must be plotted on a chart until it produces the first out-of-control signal (Montgomery, 2013). MRL could be used as a performance measure in detecting the shift size  $\tau$ , whereas the EMRL is used for detecting the shift range.

In the current literature, the research on MCV charts based on MRL is very limited. Therefore, only the synthetic MCV chart of Lee et al. (2020) based on MRL is introduced. Although the advanced chart, the synthetic MCV chart, performed better than the Shewhart MCV chart, this proposed chart can be used by the practitioner who likes to implement an intermediate-type chart in the process monitoring. This intermediate framework is simple yet effective in terms of costs and time. However, the synthetic MCV chart was not investigated in terms of EMRL, which is required to be used when the exact shift size could not be defined in certain processes. Additionally, the synthetic chart is ineffective in detecting the downward process shifts. The downward process shifts are crucial since it shows process improvement. The proposed chart circumvents these drawbacks as it has been developed and can effectively detect the upward and downward process shifts in the MRL and EMRL criteria. Figure 1 illustrates the graphical view of the proposed upward and downward charts. This paper's organization is shown as follows: The properties and distribution of the Shewhart MCV chart are discussed in Methods. Methods also enumerated the formulas and algorithms of MRL and EMRL. Then, the outputs of the proposed chart are shown in the Results and Discussion. Lastly, the concluding remarks and recommendations will be presented in Conclusion.

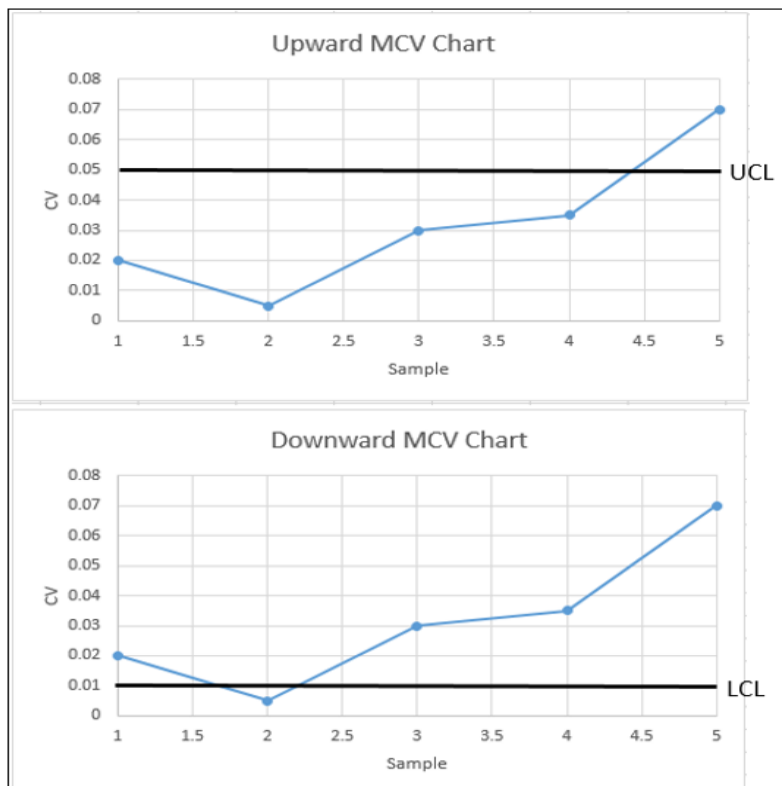


Figure 1. Graphical view of the Shewhart MCV charts

**METHODS**

According to Voinov and Nikulin (1996), suppose that we have a random sample size of  $a$ , i.e.,  $X_1, X_2, \dots, X_a$  from a  $b$ -variate normal distribution with a mean vector  $\mu$  and covariance matrix  $\Sigma$ , it gives  $X \sim N_b(\mu, \Sigma)$ , where  $X_i^T = (X_{i1}, X_{i2}, \dots, X_{ib})$ , for  $1 \leq i \leq a$  and  $\mu^T = (\mu_1, \mu_2, \dots, \mu_b)$ . The MCV statistic for the population can be denoted as  $\gamma = (\mu^T \Sigma^{-1} \mu)^{-1/2}$ . The sample MCV can assume  $\gamma, \hat{\gamma}$  if  $\mu$  and  $\Sigma$  are unknown. Thus,  $\hat{\gamma} = (\bar{X}^T S^{-1} \bar{X})^{-1/2}$  can be obtained by substituting  $\mu$  and  $\Sigma$  to  $\bar{X}$  and  $S$ . Note that  $\bar{X}$  is the sample mean vector while  $S$  is the sample covariance matrix. The  $\bar{X}$  and  $S$  are defined as  $\bar{X} = 1/a \Sigma X_i$  and  $S = 1/(a - 1) \Sigma (X_t - \bar{X})(X_t - \bar{X})^T$ , respectively. Here,  $\bar{X}$  and  $S$  are not correlated.

Based on Wijsman’s theorem (1957), Yeong et al. (2016) gave  $\hat{\gamma}$  distribution.  $\bar{X}$  is normally distributed with mean  $\mu$  and covariance matrix  $(1/a)\Sigma$ , i.e.,  $\bar{X} \sim N_b(\mu, (1/a)\Sigma)$ . At the same time,  $S$  has a Wishart distribution with  $(a - 1)$  degree of freedom and covariance matrix  $(1/(1 - a))\Sigma$ , which gives  $S \sim W_b(a - 1, (1/(a - 1))\Sigma)$ . By letting  $T^2 = a\bar{X}^T S^{-1} \bar{X}$ , it provides  $T^2/(a - 1) \cdot (a - b)/b \sim F_{b,a-b}(\delta)$ , which can be defined as a noncentral  $F$  distribution. Here,  $a$  refers to sample size, and  $b$  is the number of quality characteristics. Note that it is with  $b$  and  $a - b$  degrees of freedom and noncentrality parameter  $\delta = a\mu^T \Sigma^{-1} \mu$ . From  $\hat{\gamma} = (\bar{X}^T S^{-1} \bar{X})^{-1/2}$ , it can be further derived as by adding  $a$  to both sides. By adopting, it gives Equation 1

$$\left(\frac{\sqrt{a}}{\hat{\gamma}}\right)^2 \cdot \frac{a-b}{b} = \frac{a(a-b)}{(a-1)b\hat{\gamma}^2} \sim F_{b,a-b}(\delta). \tag{1}$$

Since  $\delta = a\mu^T \Sigma^{-1} \mu$  and it can also be formulated as  $\frac{a}{\gamma^2}$ , where  $\gamma$  is the MCV, as mentioned in the early paragraph. The cumulative distribution function (CDF) of  $\hat{\gamma}$  can be derived as Equation 2

$$\begin{aligned} F_{\hat{\gamma}}(x|a, b, \delta) &= P(\hat{\gamma} \leq x) = P\left(\frac{1}{\hat{\gamma}} \geq \frac{1}{x}\right) = P\left(\frac{a(a-b)}{(a-1)b\hat{\gamma}^2} \geq \frac{a(a-b)}{(a-1)bx^2}\right) \\ &= 1 - F_F\left(\frac{a(a-b)}{(a-1)bx^2} \mid b, a-b, \delta\right) \end{aligned} \tag{2}$$

where  $F_F(\cdot | a, a - b, \delta)$  is the noncentral  $F$  distribution. Note that it is with  $b$  and  $a - b$  degrees of freedom and noncentrality parameter  $\delta$ .

To formulate the inverse CDF of  $\hat{\gamma}$ , Yeong et al. (2016) let  $F_{\hat{\gamma}}^{-1}(\alpha|a, b, \delta) = y$  gives  $F_{\hat{\gamma}}^{-1}(y|a, b, \delta) = \alpha$ . Then, Equation 3 gives

$$1 - F_F\left(\frac{a(a-b)}{(a-1)by^2} \mid b, a-b, \delta\right) = \alpha. \tag{3}$$

Then, it gives Equation 4

$$\frac{a(a-b)}{(a-1)by^2} = F_F^{-1}(1 - \alpha|b, a - b, \delta). \tag{4}$$

With some algebraic manipulations, it provides Equation 5 as follows:

$$y = \sqrt{\frac{a(a-b)}{(a-1)b} \left[ \frac{1}{F_F^{-1}(1-\alpha|b, a-b, \delta)} \right]}, \tag{5}$$

Since  $F_{\hat{\gamma}}^{-1}(\alpha|a, b, \delta) = y$ , then the inverse CDF of can be derived in Equation 6

$$F_{\hat{\gamma}}^{-1}(\alpha|a, b, \delta) = \sqrt{\frac{a(a-b)}{(a-1)b} \left[ \frac{1}{F_F^{-1}(1-\alpha|b, a-b, \delta)} \right]}, \tag{6}$$

where  $F_F(\cdot | a, a - b, \delta)$  is the inverse CDF of the noncentral  $F$  distribution. Note that it is with  $b$  and  $a - b$  degrees of freedom and noncentrality parameter  $\delta$ . The distribution of  $\hat{\gamma}$  is only considered true when  $b < a$  due to the positive degree of freedom. Next,  $\delta = a\mu^T \Sigma^{-1} \mu$  as mentioned in the early paragraph, it is equivalent to  $\delta = a/(\tau\gamma_0)^2$ , where the shift size  $\tau = 1$  in the in-control process and  $\gamma_1 = \tau\gamma_0$  is an out-of-control MCV when  $\tau \neq 1$ . When  $\tau \neq 1$ , the values of  $\tau > 1$  and  $0 < \tau < 1$  are for an increase and decrease MCV shifts, respectively.

According to Yeong et al. (2016), the root mean square method can be applied when the in-control sample MCV, i.e.,  $\hat{\gamma}_0$ , is unknown. Then, the formula can be obtained as Equation 7:

$$\hat{\gamma}_0 = \sqrt{\frac{1}{m} \sum_{i=1}^m \hat{\gamma}_t^2}, \tag{7}$$

where  $m$  is the number of in-control Phase I samples. The two one-sided Shewhart MCV charts consist of two independent charts: the upward Shewhart MCV chart for detecting the increase of the process MCV shifts and the downward Shewhart MCV chart for detecting the decrease of the process MCV shifts. The upward chart has an upper control limit (UCL), while the downward chart has a lower control limit (LCL). The chart will detect an out-of-control signal if the sample MCV falls beyond the LCL and UCL. Therefore, the practitioner needs to identify the assignable cause(s) immediately to bring the process back to normal. By setting the Type I error probability ( $\alpha$ ), the UCL and LCL's formulas are shown in Equations 8 and 9.

$$UCL = F_{\hat{\gamma}}^{-1}(1 - \alpha|a, b, \delta_0), \tag{8}$$

for the increasing case and

$$LCL = F_{\hat{\gamma}}^{-1}(\alpha|a, b, \delta_0), \tag{9}$$

for the decreasing case. Note that  $\delta_0 = a/\gamma_0^2$  and  $\alpha = 1/ARL_0$ . The  $ARL_0$  is the in-control ARL value, where the  $ARL_0$  value is specified by the practitioner, depending on the current process system. For example, if the  $ARL_0$  is set as 370, then the  $\alpha$  value will be computed as  $\alpha = 1/370 = 0.0027$ .

As mentioned above, the process is out-of-control when the sample falls above the UCL of the upward Shewhart MCV chart and below the LCL of the downward Shewhart MCV chart. Thus, the probabilities that the upward and downward Shewhart MCV charts for detecting an out-of-control signal are  $Q = Pr(\hat{y} > UCL)$  and  $Q = Pr(\hat{y} < LCL)$ , respectively. Subsequently, the ARL and expected ARL (EARL) are shown in Equations 10 and 11:

$$ARL = \frac{1}{Q} \tag{10}$$

and

$$EARL = \int_{\tau_{min}}^{\tau_{max}} ARL_1 f_{\tau}(\tau) d\tau \tag{11}$$

where  $ARL_1$  is an out-of-control ARL and  $f_{\tau}(\tau)$  denotes the probability density function (PDF) of  $\tau$ . According to Yeong et al. (2016), the EARL is a better performance measure for the case when  $\tau$  unable to be specified by the practitioner. In the interval  $(\tau_{max}, \tau_{min})$ , the  $\tau_{min}$  is the lower bound of  $\tau$ , whereas the  $\tau_{max}$  is the upper bound of  $\tau$ , subject to  $\tau_{max} > \tau_{min}$ .

The limits of the charts are known constants if the plotted statistics are independent (Montgomery, 2013). Thus, the probability mass function (PMF), that is,  $f_{RL}(l)$  and CDF, that is,  $F_{RL}(l)$  of the run length (RL) for the Shewhart MCV chart, can be obtained as  $f_{RL}(l) = P(RL = l) = \alpha(1 - \alpha)^{l-1}$  and  $F_{RL}(l) = P(RL \leq l) = 1 - (1 - \alpha)^l$ , respectively, where  $l \in \{1, 2, 3, \dots\}$ . According to Gan (1993), the  $(100\theta)^{th}$  percentile of the run-length distribution can be denoted as the value  $l_{\theta}$  such as in Equation 12

$$P(RL \leq l_{\theta} - 1) \leq \theta \text{ and } P(RL \leq l_{\theta}) > \theta. \tag{12}$$

where  $0 < \theta < 1$ . Then, the percentiles of the run-length distribution of the upward and downward Shewhart MCV charts can be computed such that MRL, by setting  $\theta = 0.5$  in Equation (12), that is,  $P(RL \leq MRL - 1) \leq 0.5$  and  $P(RL \leq MRL) > 0.5$ . Note that the practitioner can specify the in-control MRL ( $MRL_0$ ) based on the current process system. When the shift size  $\tau$  is unknown, the EMRL can be used as the performance measure. For the computation of EMRL, the formula is shown in Equation 13

$$EMRL = \int_{\tau_{min}}^{\tau_{max}} MRL f_{\tau}(\tau) d\tau \tag{13}$$

where the in-control EMRL ( $EMRL_0$ ) is equal to the  $MRL_0$  and  $f_{\tau}(\tau)$  is the PDF of  $\tau$ .

## RESULTS AND DISCUSSION

Tables 1, 2, and 3 present the  $(\vartheta_{0.05}, \text{MRL}_1, \vartheta_{0.95})$  values for the upward and downward Shewhart MCV charts for monitoring the upward and downward MCV shifts, respectively, when  $b \in \{2, 3, 4\}$ ,  $a \in \{5, 10, 15\}$ ,  $\gamma_0 \in \{0.1, 0.5\}$ ,  $\tau \in \{1.1, 1.2, 1.3, 1.4, 1.5\}$  (for the upward case) and  $\tau \in \{0.5, 0.6, 0.7, 0.8, 0.9\}$  (for the downward case) and the  $\text{MRL}_0$  value is specified as 250 (when  $\tau = 1.0$ ). Note that the values of sample size  $a$  and the quality characteristics  $b$  were adopted from Yeong et al. (2016) and Khatun et al. (2019). The spread and variation of the run-length distribution can be measured by referring to the difference of the values between  $\vartheta_{0.05}$  and  $\vartheta_{0.95}$ , where  $\vartheta_{0.05}$  and  $\vartheta_{0.95}$  are the 5<sup>th</sup> and 95<sup>th</sup> percentiles of the run-length distribution, respectively. The results reveal that the larger shift  $\tau$  gives smaller  $(\vartheta_{0.05}, \text{MRL}_1, \vartheta_{0.95})$  values with any change of the  $b$ ,  $\gamma_0$ , and  $n$  values. For example, in Table 1, for  $b = 2$ ,  $\gamma_0 = 0.1$  and  $a = 10$ , the  $\text{MRL}_1 \in \{(6, 81, 347), (2, 18, 76), (1, 7, 30)\}$  when upward shift  $\tau \in \{1.1, 1.3, 1.5\}$  whereas the  $\text{MRL}_1 \in \{(15, 190, 820), (8, 97, 417), (3, 38, 163)\}$  when downward shift  $\tau \in \{0.9, 0.7, 0.5\}$ .

The run-length distribution's variation is inversely proportional to the shift size. It shows that the variation decreases if the shift size increases. One of the examples is shown in Table 2; for  $b = 3$ ,  $\gamma_0 = 0.5$ , and  $a = 5$ , the different values between  $\vartheta_{0.05}$  and  $\vartheta_{0.95}$  are (454, 143, 69) when  $\tau \in \{1.1, 1.3, 1.5\}$  (for upward shift) and (887, 557, 296) when  $\tau \in \{0.9, 0.7, 0.5\}$  (for downward shift). The  $(\vartheta_{0.05}, \text{MRL}_1, \text{and } \vartheta_{0.95})$  values have a minimal decrease trend for detecting the downward shift with a small sample size value,  $a = 5$ . For example, in Table 3, for  $b = 4$ ,  $\gamma_0 = 0.1$ , and  $a = 5$ , the decreased percentage of the  $\text{MRL}_1$  value from  $\tau = 0.9$  to  $\tau = 0.5$  is 46% while the decreased percentages when  $a = 10$  and 15 are 92% and 98%, respectively. Generally, the  $(\vartheta_{0.05}, \text{MRL}_1, \text{and } \vartheta_{0.95})$  values increase when  $b$  and  $\gamma_0$  values increase. An example is presented in Tables 1, 2, and 3, for  $b \in \{2, 3, 4\}$ ,  $a = 5$  and  $\tau = 1.1$ , the  $\text{MRL}_1 \in \{(81, 97), (91, 107), (107, 123)\}$ , when  $\gamma_0 \in \{0.1, 0.5\}$ .

In terms of the  $\text{EMRL}_1$  criterion, Tables 4, 5, and 6 present the values for the upward and downward Shewhart MCV charts, for monitoring the upward and downward MCV shift ranges, respectively, when  $b \in \{2, 3, 4\}$ ,  $a \in \{5, 10, 15\}$ ,  $\gamma_0 \in \{0.1, 0.5\}$ ,  $(\tau \max_{\min} \epsilon) \in \{(1.0, 2.0), (1.3, 2.0), (1.5, 2.0)\}$  (for the upward case) and  $(\tau \max_{\min} \epsilon) \in \{(0.3, 1.0), (0.5, 1.0), (0.7, 1.0)\}$  (for the downward case) and the  $\text{EMRL}_0$  value is set equal to the  $\text{MRL}_0$  value, that is 250. Generally, the detected trend on the effect of  $b$ ,  $a$ , and  $\gamma_0$  values is nothing different from the case of  $\text{MRL}_1$ . However, it shows that the run-length distribution's variation for the downward shift ranges is larger than the run-length distribution's, regardless of the  $b$ ,  $\gamma_0$ , and  $a$  values. For instance, in Table 4, when  $b = 2$ ,  $a = 5$ , and  $\gamma_0 = 0.1$ , the run-length distribution's variation of the downward shift range  $(\tau \max_{\min} \epsilon) (0.5, 1.0)$  is 531.23 while the upward shift range  $(\tau \max_{\min} \epsilon) (1.0, 2.0)$  is 111.12. Note that the shift ranges (0.5, 1.0) and (1.0, 2.0) are considered very practical in the real industry (Castagliola et al., 2011).

Table 1

$(\vartheta_{0.05}, MRL_1, \vartheta_{0.95})$  values of the two one-sided Shewhart MCV charts, for the case  $b = 2$ ,  $a \in \{5, 10, 15\}$ ,  $\gamma_0 \in \{0.1, 0.5\}$ ,  $\tau \in \{0.5, 0.6, 0.7, 0.8, 0.9, 1.1, 1.2, 1.3, 1.4, 1.5\}$  and  $MRL_0 = 250$

$\tau$	$\gamma_0 = 0.1$	$\gamma_0 = 0.5$
$a = 5$		
0.5	3, 38, 163	3, 38, 164
0.6	5, 63, 273	5, 63, 272
0.7	8, 97, 417	8, 97, 416
0.8	11, 140, 602	11, 138, 597
0.9	15, 190, 820	15, 191, 825
1.1	6, 81, 347	8, 97, 418
1.2	3, 35, 148	4, 48, 204
1.3	2, 18, 76	2, 27, 117
1.4	1, 11, 45	2, 18, 75
1.5	1, 7, 30	1, 13, 53
$a = 10$		
0.5	1, 5, 18	1, 5, 20
0.6	1, 12, 50	1, 13, 53
0.7	3, 29, 126	3, 30, 129
0.8	5, 67, 287	5, 66, 284
0.9	10, 135, 583	10, 134, 576
1.1	5, 55, 237	6, 71, 307
1.2	2, 19, 79	3, 29, 122
1.3	1, 9, 35	2, 14, 61
1.4	1, 5, 19	1, 9, 36
1.5	1, 3, 12	1, 6, 23
$a = 15$		
0.5	1, 2, 6	1, 2, 7
0.6	1, 5, 18	1, 5, 20
0.7	1, 14, 58	1, 14, 59
0.8	4, 41, 177	3, 39, 168
0.9	9, 113, 489	8, 103, 445
1.1	4, 43, 183	5, 58, 248
1.2	1, 13, 53	2, 20, 87
1.3	1, 5, 22	1, 10, 40
1.4	1, 3, 12	1, 6, 22
1.5	1, 2, 7	1, 4, 14

Table 2

$(\vartheta_{0.05}, MRL_1, \vartheta_{0.95})$  values of the two one-sided Shewhart MCV charts, for the case  $b = 3$ ,  $a \in \{5, 10, 15\}$ ,  $\gamma_0 \in \{0.1, 0.5\}$ ,  $\tau \in \{0.5, 0.6, 0.7, 0.8, 0.9, 1.1, 1.2, 1.3, 1.4, 1.5\}$  and  $MRL_0 = 250$

$\tau$	$\gamma_0 = 0.1$	$\gamma_0 = 0.5$
$a = 5$		
0.5	6, 69, 297	6, 70, 301
0.6	8, 98, 422	8, 99, 426
0.7	10, 131, 563	10, 132, 567
0.8	13, 168, 724	13, 168, 723
0.9	16, 207, 891	16, 209, 903
1.1	7, 91, 391	8, 107, 462
1.2	4, 42, 180	5, 56, 242
1.3	2, 23, 98	3, 34, 146
1.4	2, 14, 60	2, 23, 98
1.5	1, 10, 41	2, 17, 71
$a = 10$		
0.5	1, 6, 26	1, 7, 28
0.6	2, 16, 67	2, 17, 70
0.7	3, 36, 156	3, 37, 158
0.8	6, 76, 329	6, 76, 325
0.9	11, 144, 620	11, 143, 614
1.1	5, 59, 252	6, 75, 324
1.2	2, 21, 88	3, 31, 134
1.3	1, 10, 40	2, 16, 68
1.4	1, 5, 22	1, 10, 41
1.5	1, 4, 14	1, 7, 27
$a = 15$		
0.5	1, 2, 7	1, 2, 8
0.6	1, 5, 22	1, 6, 23
0.7	2, 16, 68	2, 16, 68
0.8	4, 46, 197	4, 43, 186
0.9	9, 119, 513	8, 109, 468
1.1	4, 45, 192	5, 60, 258
1.2	1, 14, 57	2, 22, 93
1.3	1, 6, 24	1, 10, 43
1.4	1, 3, 13	1, 6, 24
1.5	1, 2, 8	1, 4, 16

Table 3

$(\vartheta_{0.05}, MRL_1, \vartheta_{0.95})$  values of the two one-sided Shewhart MCV charts, for the case  $b = 4$ ,  $a \in \{5, 10, 15\}$ ,  $\gamma_0 \in \{0.1, 0.5\}$ ,  $\tau \in \{0.5, 0.6, 0.7, 0.8, 0.9, 1.1, 1.2, 1.3, 1.4, 1.5\}$  and  $MRL_0 = 250$

$\tau$	$\gamma_0 = 0.1$	$\gamma_0 = 0.5$
$a = 5$		
0.5	9, 122, 526	10, 131, 564
0.6	12, 149, 644	12, 156, 673
0.7	13, 175, 754	14, 180, 778
0.8	15, 201, 868	16, 204, 878
0.9	17, 225, 970	17, 229, 990
1.1	8, 107, 461	10, 123, 530
1.2	5, 55, 238	6, 71, 306
1.3	3, 33, 141	4, 46, 199
1.4	2, 22, 92	3, 33, 141
1.5	2, 15, 65	2, 25, 106
$a = 10$		
0.5	1, 9, 38	1, 10, 41
0.6	2, 22, 92	2, 22, 95
0.7	4, 46, 197	4, 46, 197
0.8	7, 88, 380	7, 87, 375
0.9	12, 153, 661	12, 153, 658
1.1	5, 63, 270	6, 80, 334
1.2	2, 23, 98	3, 34, 147
1.3	1, 11, 46	2, 18, 77
1.4	1, 6, 25	1, 11, 47
1.5	1, 4, 16	1, 8, 31
$a = 15$		
0.5	1, 2, 9	1, 3, 10
0.6	1, 7, 27	1, 7, 28
0.7	2, 19, 80	2, 19, 79
0.8	4, 51, 220	4, 48, 206
0.9	10, 125, 539	9, 114, 493
1.1	4, 47, 202	5, 63, 270
1.2	2, 15, 62	2, 23, 99
1.3	1, 6, 26	1, 11, 47
1.4	1, 4, 14	1, 7, 27
1.5	1, 2, 9	1, 4, 17

Table 4

$(E\vartheta_{0.05}, EMRL_1, E\vartheta_{0.95})$  values of the two one-sided Shewhart MCV charts, for the case  $b = 2, a \in \{5, 10, 15\}$ ,  $\gamma_0 \in \{0.1, 0.5\}$ ,  $(\tau_{max_{min}} \in) \{(0.3, 1.0), (0.5, 1.0), (0.7, 1.0), (1.0, 2.0), (1.3, 2.0), (1.5, 2.0)\}$  and  $EMRL_0 = 250$

$(\tau_{max_{min}})$	$\gamma_0 = 0.1$	$\gamma_0 = 0.5$
$a = 5$		
(0.3, 1.0)	7.61, 96.57, 420.90	7.61, 96.47, 420.32
(0.5, 1.0)	9.84, 125.68, 541.07	8.84, 125.98, 542.66
(0.7, 1.0)	12.95, 167.40, 722.03	12.82, 166.73, 719.32
(1.0, 2.0)	2.60, 26.65, 113.72	2.93, 33.61, 143.56
(1.3, 2.0)	1.05, 6.25, 24.71	1.25, 10.46, 43.83
(1.5, 2.0)	1.00, 4.07, 15.63	1.00, 7.32, 30.12
$a = 10$		
(0.3, 1.0)	4.47, 52.60, 238.93	4.38, 52.37, 237.85
(0.5, 1.0)	5.81, 71.77, 317.32	5.72, 71.39, 315.63
(0.7, 1.0)	8.67, 111.06, 477.52	8.57, 109.71, 471.99
(1.0, 2.0)	2.08, 18.74, 79.92	2.34, 23.86, 101.57
(1.3, 2.0)	1.00, 2.69, 10.29	1.01, 5.10, 19.70
(1.5, 2.0)	1.00, 1.82, 5.99	1.00, 3.31, 12.41
$a = 15$		
(0.3, 1.0)	3.70, 42.01, 193.12	3.48, 39.80, 182.16
(0.5, 1.0)	4.68, 56.88, 256.35	4.47, 54.46, 244.51
(0.7, 1.0)	7.17, 91.05, 393.88	6.83, 86.27, 372.57
(1.0, 2.0)	1.85, 15.67, 66.01	2.12, 19.84, 83.54
(1.3, 2.0)	1.00, 1.77, 6.20	1.00, 3.21, 12.36
(1.5, 2.0)	1.00, 1.25, 3.75	1.00, 2.13, 7.64

Table 5

$(E\vartheta_{0.05}, EMRL_1, E\vartheta_{0.95})$  values of the two one-sided Shewhart MCV charts, for the case  $b = 3, a \in \{5, 10, 15\}, \gamma_0 \in \{0.1, 0.5\}, (\tau_{max_{min}}) \in \{(0.3, 1.0), (0.5, 1.0), (0.7, 1.0), (1.0, 2.0), (1.3, 2.0), (1.5, 2.0)\}$  and  $EMRL_0 = 250$

$(\tau_{max_{min}})$	$\gamma_0 = 0.1$	$\gamma_0 = 0.5$
$a = 5$		
(0.3, 1.0)	9.57, 122.04, 526.11	9.57, 122.81, 529.84
(0.5, 1.0)	11.72, 151.33, 652.63	11.85, 153.24, 659.99
(0.7, 1.0)	14.25, 188.35, 812.95	14.35, 188.89, 814.78
(1.0, 2.0)	2.78, 30.46, 130.06	3.25, 38.65, 165.16
(1.3, 2.0)	1.17, 8.27, 33.69	1.40, 14.05, 59.10
(1.5, 2.0)	1.00, 5.54, 22.12	1.10, 10.22, 42.25
$a = 10$		
(0.3, 1.0)	4.66, 57.12, 258.07	4.68, 57.01, 257.60
(0.5, 1.0)	6.11, 77.91, 342.67	6.05, 77.82, 340.83
(0.7, 1.0)	9.26, 118.66, 510.99	9.19, 117.31, 505.26
(1.0, 2.0)	2.12, 19.85, 84.13	2.52, 25.27, 107.39
(1.3, 2.0)	1.00, 3.05, 11.78	1.05, 5.54, 22.74
(1.5, 2.0)	1.00, 2.01, 7.05	1.00, 3.72, 14.60
$a = 15$		
(0.3, 1.0)	3.74, 43.97, 202.12	3.63, 41.67, 190.67
(0.5, 1.0)	4.98, 59.72, 268.37	4.76, 57.07, 255.77
(0.7, 1.0)	7.55, 94.95, 410.73	7.08, 90.09, 388.48
(1.0, 2.0)	1.88, 16.11, 68.18	2.12, 20.37, 86.76
(1.3, 2.0)	1.00, 1.87, 6.89	1.00, 3.59, 13.45
(1.5, 2.0)	1.00, 1.25, 4.09	1.00, 2.43, 8.33

Table 6

values of the two one-sided Shewhart MCV charts, for the case  $b = 4$ ,  $a \in \{5, 10, 15\}$ ,  $\gamma_0 \in \{0.1, 0.5\}$ ,  $(\tau_{max_{min}} \epsilon) \in \{(0.3, 1.0), (0.5, 1.0), (0.7, 1.0), (1.0, 2.0), (1.3, 2.0), (1.5, 2.0)\}$  and  $EMRL_0 = 250$

$(\tau_{max_{min}})$	$\gamma_0 = 0.1$	$\gamma_0 = 0.5$
$a = 5$		
(0.3, 1.0)	12.44, 161.48, 696.08	12.83, 167.38, 722.30
(0.5, 1.0)	14.12, 185.83, 801.75	14.74, 191.94, 827.81
(0.7, 1.0)	16.23, 213.75, 922.54	16.45, 216.25, 932.47
(1.0, 2.0)	3.25, 37.64, 160.67	3.96, 47.56, 203.77
(1.3, 2.0)	1.40, 12.81, 53.86	2.05, 21.11, 89.67
(1.5, 2.0)	1.05, 8.93, 37.05	1.64, 15.95, 67.71
$a = 10$		
(0.3, 1.0)	5.16, 63.13, 283.50	5.08, 63.04, 282.84
(0.5, 1.0)	6.88, 85.88, 374.46	6.76, 85.79, 372.81
(0.7, 1.0)	9.94, 128.07, 550.78	9.94, 126.53, 545.17
(1.0, 2.0)	2.24, 20.90, 89.15	2.59, 26.81, 114.32
(1.3, 2.0)	1.00, 3.60, 13.74	1.05, 6.39, 26.29
(1.5, 2.0)	1.00, 2.35, 8.24	1.00, 4.37, 17.33
$a = 15$		
(0.3, 1.0)	3.95, 46.27, 212.28	3.78, 43.92, 200.62
(0.5, 1.0)	5.08, 62.89, 281.90	4.88, 60.08, 268.82
(0.7, 1.0)	7.84, 99.56, 429.86	7.62, 94.44, 406.90
(1.0, 2.0)	1.95, 16.70, 70.83	2.24, 21.30, 90.03
(1.3, 2.0)	1.00, 2.13, 7.40	1.00, 3.72, 14.80
(1.5, 2.0)	1.00, 1.35, 4.49	1.00, 2.62, 9.16

## CONCLUSION

No attempt has been made to investigate the Shewhart MCV chart based on MRL and EMRL in the current literature. This paper proposes the two one-sided Shewhart MCV charts for monitoring the upward and downward MCV shifts and shift ranges based on MRL and EMRL. In the existing literature, the ARL performance measure should not be the only measure as it could potentially cause the chart's misinterpretation. The ARL performance measure may not be practically effective due to the inconsistency and excessive variations of the run-length distribution. It shows the importance of this study, in which the proposed charts can circumvent the drawbacks of using ARL, and at the same time, the biased performance of the two-sided MCV chart can be resolved. Additionally, the proposed

charts can be used by the practitioner who likes to implement an intermediate-type chart in the process monitoring. This intermediate framework is simple yet effective in terms of costs and time. The proposed charts provided the results based on the  $MRL_1$  and  $EMRL_1$  criteria. The variation and spread of the run-length distribution are discussed by referring to the run-length distribution's 5<sup>th</sup> and 95<sup>th</sup> percentiles. The effects of different parameter combinations on the proposed chart's performance are the sample size  $a$ , the number of quality characteristics  $b$ , the in-control MCV value  $\gamma_0$ , the MCV shifts (for MRL), and the MCV shift ranges (for EMRL) are investigated. The proposed charts can be investigated in the future by including measurement errors. It can help the practitioner obtain more accurate results when implementing the proposed charts in real-life manufacturing, healthcare, service, and finance processes.

## ACKNOWLEDGMENT

The Universiti Sains Malaysia supports this work, Short Term Grant [Grant Number: 304 / PKOMP / 6315616], with the project entitled "New Coefficient of Variation Control Charts based on Variable Charting Statistics in Industry 4.0 for the Quality Smart Manufacturing and Services."

## REFERENCES

- Adegoke, N. A., Dawod, A., Adeoti, O. A., Sanusi, R. A. & Abbasi, S. A. (2022). Monitoring the multivariate coefficient of variation for high dimensional processes. *Quality and Reliability Engineering International*, 38(5), 2606-2621. <https://doi.org/10.1002/qre.3094>
- Alharbi, S., Raun, W. R., Arnall, D. B., & Zhang, H. (2019). Prediction of maize (*Zea mays* L.) population using normalized-difference vegetative index (NDVI) and coefficient of variation (CV). *Journal of Plant Nutrition*, 42, 673-679. <https://doi.org/10.1080/01904167.2019.1568465>
- Calzada, M. E., & Scariano, S. M. (2013). A synthetic control chart for the coefficient of variation. *Journal of Statistical Computation and Simulation*, 83, 853-867. <https://doi.org/10.1080/00949655.2011.639772>
- Castagliola, P., Achouri, A., Taleb, H., Celano, G., & Psarakis, P. (2013). Monitoring the coefficient of variation using control charts with run rules. *Quality Technology & Quantitative Management*, 10, 75-94. <https://doi.org/10.1080/16843703.2013.11673309>
- Castagliola, P., Achouri, A., Taleb, H., Celano, G., & Psarakis, P. (2015). Monitoring the coefficient of variation using a variable sample size control chart. *The International Journal of Advanced Manufacturing Technology*, 80, 1561-1576. <https://doi.org/10.1007/s00170-015-7084-4>
- Castagliola, P., Celano, G., & Psarakis, S. (2011). Monitoring the coefficient of variation using EWMA charts. *Journal of Quality Technology*, 43, 249-265. <https://doi.org/10.1080/00224065.2011.11917861>
- Chakraborti, S. (2007). Run-length distribution and percentiles: The Shewhart  $\bar{X}$  chart with unknown parameters. *Quality Engineering*, 19, 119-127. <https://doi.org/10.1080/08982110701276653>

- Chanda, S., Kanke, Y., Dalen, M., Hoy, J., & Tubana, B. (2018). Coefficient of variation from vegetarian index for sugarcane population and stalk evaluation. *Agrosystems, Geosciences & Environment*, 1, 1-9. <https://doi.org/10.2134/age2018.07.0016>
- Chew, M. H., Yeong, W. C., Talib, M. A., Lim, S. L., & Khaw, K. W. (2021). Evaluating the steady-state performance of the synthetic coefficient of variation chart. *Pertanika Journal of Science and Technology*, 29(3), 2149-2173. <https://doi.org/10.47836/pjst.29.3.20>
- Chew, X. Y., Khaw, K. W., & Yeong, W. C. (2020). The efficiency of run rules schemes for the multivariate coefficient of variation: A Markov chain approach. *Journal of Applied Statistics*, 47, 460-480. <https://doi.org/10.1080/02664763.2019.1643296>
- Chew, X. Y., Khoo, M. B. C., Khaw, K. W., Yeong, W. C., & Chong, Z. L. (2019). A proposed variable parameter control chart for monitoring the multivariate coefficient of variation. *Quality and Reliability Engineering International*, 35, 2442-2461. <https://doi.org/10.1002/qre.2536>
- Doughty, M. J., & Aakre, B. M. (2008). Further analysis of assessments of the coefficient of variation of corneal endothelial cell areas from specular microscopic images. *Clinical and Experimental Optometry*, 91, 438-446. <https://doi.org/10.1111/j.1444-0938.2008.00281.x>
- Gan, F. F. (1993). An optimal design of EWMA control charts based on median run length. *Journal of Statistical Computation and Simulation*, 45, 169-184. <https://doi.org/10.1080/00949659308811479>
- Giner-Bosch, V., Tran, K. P., Castagliola, P., & Khoo, M. B. C. (2019). An EWMA control chart for the multivariate coefficient of variation. *Quality and Reliability Engineering International*, 35, 1515-1541. <https://doi.org/10.1002/qre.2459>
- Huang, C. C., & Tang, T. (2007). Development of a new infrared device for monitoring the coefficient of variation in yarns. *Journal of Applied Polymer Science*, 106, 2342-2349. <https://doi.org/10.1002/app.25441>
- Kang, C. W., Lee, M. S., Seong, Y. J., & Hawkins, D. M. (2007). A control chart for the coefficient of variation. *Journal of Quality Technology*, 39, 151-158. <https://doi.org/10.1080/00224065.2007.11917682>
- Khatun, M., Khoo, M. B. C., Lee, M. H., & Castagliola, P. (2019). One-sided control charts for monitoring the coefficient of variation in short production runs. *Transactions of the Institute of Measurement and Control*, 41, 1712-1728. <https://doi.org/10.1177/0142331218789481>
- Khaw, K. W., & Chew, X. Y. (2019). A re-evaluation of the run rules control charts for monitoring the coefficient of variation. *Statistics, Optimization & Information Computing*, 7, 716-730. <https://doi.org/10.19139/soic-2310-5070-717>
- Khaw, K. W., Chew, X. Y., Lee, M. H., & Yeong, W. C. (2021). An optimal adaptive variable sample size scheme for the multivariate coefficient of variation. *Statistics, Optimization & Information Computing*, 9, 681-693. <https://doi.org/10.19139/soic-2310-5070-996>
- Khaw, K. W., Chew, X. Y., Yeong, W. C., & Lim, S. L. (2019). Optimal design of the synthetic control chart for monitoring the multivariate coefficient of variation. *Chemometrics and Intelligent Laboratory Systems*, 186, 33-40. <https://doi.org/10.1016/j.chemolab.2019.02.001>
- Khaw, K. W., Khoo, M. B. C., Castagliola, P., & Rahim, M. A. (2018). New adaptive control charts for monitoring the multivariate coefficient of variation. *Computers & Industrial Engineering*, 126, 595-610. <https://doi.org/10.1016/j.cie.2018.10.016>

- Khaw, K. W., Khoo, M. B. C., Yeong, W. C., & Wu, Z. (2017). Monitoring the coefficient of variation using a variable sample size and sampling interval control chart. *Communications in Statistics - Simulation and Computation*, *46*, 5772-5794. <https://doi.org/10.1080/03610918.2016.1177074>
- Khoo, M. B. C., Wong, V. H., Wu, Z., & Castagliola, P. (2012). Optimal design of the synthetic chart for the process mean based on median run length. *IIE Transactions*, *44*, 765-779. <https://doi.org/10.1080/0740817X.2011.609526>
- Lee, M. H., Lim, V. Y. C., Chew, X. Y., Lau, M. F., Yakub, S., & Then, P. H. H. (2020). Design of the synthetic multivariate coefficient of variation chart based on the median run length. *Advances in Mathematics: Scientific Journal*, *9*, 7397-7406. <https://doi.org/10.37418/amsj.9.9.86>
- Lim, S. L., Yeong, W. C., Khoo, M. B. C., Chong, Z. L., & Khaw, K. W. (2019). An alternative design for the variable sample size coefficient of variation chart based on the median run length and expected median run length. *International Journal of Industrial Engineering: Theory, Applications, and Practice*, *26*, 199-220. <https://doi.org/10.23055/ijietap.2019.26.2.4085>
- Mahmood, T., & Abbasi, S. A. (2021). Efficient monitoring the coefficient of variation with an application to chemical reactor process. *Quality and Reliability Engineering International*, *37*, 1135-1149. <https://doi.org/10.1002/qre.2785>
- Mim, F. N., Saha, S., Khoo, M. B. C., & Khatun, M. (2019). A side-sensitive modified group runs control chart with auxiliary information to detect process mean shifts. *Pertanika Journal of Science and Technology*, *27*(2), 847-866.
- Mo, Y., Ma, X., Lu, J., Shen, Y., Wang, Y., Zhang, L., Lu, W., Zhu, W., Bao, Y., & Zhou, J. (2021). Defining the target value of the coefficient of variation by continuous glucose monitoring in Chinese people with diabetes. *Journal of Diabetes Investigation*, *12*, 1025-1034. <https://dx.doi.org/10.1111%2Fjdi.13453>
- Montgomery, D. C. (2013). *Statistical quality control: A modern introduction*. John Wiley & Sons, Inc.
- Ng, W. C., Khoo, M. B. C., Chong, Z. L., & Lee, M. H. (2022). Economic and economic-statistical designs of multivariate coefficient of variation chart. *REVSTAT-Statistical Journal*, *20*, 117-134. <https://doi.org/10.57805/revstat.v20i1.366>
- Nguyen, Q. T., Tran, K. P., Heuchenne, H. L., Nguyen, T. H., & Nguyen, H. D. (2019). Variable sampling Interval Shewhart control charts for monitoring the multivariate coefficient of variation. *Applied Stochastics Models in Business and Industry*, *35*, 1253-1268. <https://doi.org/10.1002/asmb.2472>
- Shriberg, L. D., Green, J. R., Campbell, T. F., Mcsweeny, J. L., & Scheer, A. R. (2003). A diagnostic marker for childhood apraxia of speech: The coefficient of variation ratio. *Clinical Linguistic & Phonetics*, *17*, 575-595. <https://doi.org/10.1080/0269920031000138141>
- Teoh, W. L., Chong, J. K., Khoo, M. B. C., Castagliola, P., & Yeong, W. C. (2017). Optimal designs of the variable sample size  $\bar{X}$  chart based on median run length and expected median run length. *Quality and Reliability Engineering International*, *33*, 121-134. <https://doi.org/10.1002/qre.1994>
- Tran, P. H., & Tran, K. P. (2016). The efficiency of CUSUM schemes for monitoring the coefficient of variation. *Applied Stochastic Models in Business and Industry*, *32*, 870-881. <https://doi.org/10.1002/asmb.2213>

- Voinov, V. G., & Nikulin, M. S. (1996). *Unbiased estimator and their applications, multivariate case* (2nd Ed.). Kluwer Publishing.
- Wijsman, R. A. (1957). Random orthogonal transformations and their use in some classical distribution problems in multivariate analysis. *The Annals of Mathematical Statistics*, 28, 415-423. <https://doi.org/10.1214/AOMS%2F1177706969>
- Yeong, W. C., Khoo, M. B. C., Teoh, W. L., & Castagliola, P. (2016). A control chart for the multivariate coefficient of variation. *Quality and Reliability Engineering International*, 32, 1213-1225. <https://doi.org/10.1002/qre.1828>
- Yeong, W. C., Lee, P. Y., Lim, S. L., Ng, P. S., & Khaw, K. W. (2021). Optimal designs of the side sensitive synthetic chart for the coefficient of variation based on median run length and expected median run length. *PLoS ONE*, 16, Article e0255366. <https://doi.org/10.1371/journal.pone.0255366>
- Yeong, W. C., Lim, S. L., Khoo, M. B. C., & Castagliola, P. (2018). Monitoring the coefficient of variation using a variable parameter chart. *Quality Engineering*, 30, 212-235. <https://doi.org/10.1080/08982112.2017.1310230>
- Yeong, W. C., Tan, Y. Y., Lim, S. L., Khaw, K. W., & Khoo, M. B. C. (2022). A variable sample size run sum coefficient of variation chart. *Quality and Reliability Engineering International*, 38, 1869-1885. <https://doi.org/10.1002/qre.3057>
- Zhang, J., Li, Z., Chen, B., & Wang, Z. (2014). A new exponentially weighted moving average control chart for monitoring the coefficient of variation. *Computers & Industrial Engineering*, 78, 205-212. <https://doi.org/10.1016/j.cie.2014.09.027>
- Zhou, Q., Zou, C., Wang, Z., & Jiang, W. (2012). Likelihood-based EWMA charts for monitoring Poisson count data with time-varying sample sizes. *Journal of the American Statistical Association*, 107, 1049-1062. <https://doi.org/10.1080/01621459.2012.682811>